Pergamon

Int. J. Heat Mass Transfer. Vol. 40, No. 3, pp. 605–612, 1997

0017–9310/97 $15.00+0.00

PII: S0017–9310(96)00133–0

Numerical studies on thermal convection in cold groundwater

EKKEHARD HOLZBECHER

Technical University Berlin, P.O. Box 100 320, 10563 Berlin, Germany

(*Received* 11 *October* 1995 *and in final form* 27 *March* 1996)

Abstract—Convective flow patterns in near-surface aquifers can be induced, if a critical temperature gradient with respect to the Rayleigh number is exceeded. In cold seasons the gradient is usually steeper, because the temperature at the watertable is lowered. The paper discusses the change of critical margin due to variable water properties, i.e. nonlinear changes in density and viscosity. Copyright © 1996 Elsevier Science Ltd.

1. INTRODUCTION

The classical study about porous media convection was published by Lapwood in 1948 [1], where theoretical analysis lead to the definition of the porous medium Rayleigh number (*Ra*) and its critical value of $4\pi^2$. Thermal convection under the subsurface since then has attracted much scientific interest from geothermal applications. The change of the critical value and of convective patterns has been studied as an effect of anisotropies, inhomogeneities, viscosity changes and nonlinear density changes.

Low temperatures in most of the contributions are above 20°C, a reasonable condition for many applications. Only few papers are dealing with lower temperatures, although this is the usual situation near the subsurface in winter months under moderate climatic conditions, not to speak of regions with colder climates.

Applying linear stability theory, Sun *et al.* [2] investigated the onset of convection for liquids with a density maximum. For this case the Rayleigh number is modified using the coefficients in the cubic density–temperature relationship. Unfortunately there are no hints given about the amount of change for some temperature intervals of interest.

An experimental set-up is described by Yen [3] and used to determine the relationship between *Ra* and Nusselt number (*Nu*). A dependency on temperature range could be verified experimentally for temperature intervals of more than 10°C.

A smaller temperature gradient (< 8°C) was studied by Blake *et al.* [4]. The authors use a quadratic density–temperature state equation and modify the Rayleigh number according to that function. The numerical analysis is similar to the one used in this paper, but based on a constant Prandtl number and thus on constant viscosity.

Linear stability analysis is again used by Poulikakos [5] to investigate the transient development of the system. The parameters are chosen in a way that the situation is supercritical and an initial perturbation develops into a stable convective pattern. In parts, this paper uses the same approach but the focus remains on steady state.

The following numerical experiments intend to give a picture of steady-state convection for temperature intervals of different size with lower temperatures at 0, 2 and 4°C. Viscosity changes are taken into account additionally, which have been neglected in the literature on cold water convection so far.

2. ASSUMPTIONS AND EQUATIONS

The analytical formulation of convection is based on the principles of mass and energy conservation (see for example: Combarnous and Bories [6]):

$$\frac{\partial}{\partial t}\varphi\rho = -\nabla\cdot\rho\mathbf{v} \tag{1}$$

$$\frac{\partial}{\partial t}(\rho c)^{*}T = -\nabla[(\rho c)_f\mathbf{v}T+\mathbf{j}]. \tag{2}$$

For mass and heat flux, the empirical laws of Darcy and Fourier have to be applied:

$$\mathbf{v} = -\frac{\mathbf{k}}{\mu}\nabla(p-\rho gz) \tag{3}$$

$$\mathbf{j} = -\lambda\nabla T. \tag{4}$$

As described in details by Joseph [7] the set of equations can be simplified if the Oberbeck–Boussinesq assumption is valid. The assumption is, that density differences can be neglected except from the buoyancy term (in Darcy's Law). Analytical arguments for the validity of this assumption, using different kinds of perturbation schemes, have been given by Oberbeck [8] first, Mihaljan [9] and Fife [10] later.

Concerning the numerical finite volume discretization, the Boussinesq–Oberbeck assumption

NOMENCLATURE

D	thermal diffusivity ($\lambda/(\rho c)^*$)
f_μ	correction factor due to viscosity change
f_ρ	correction factor due to nonlinear density change
g	constant of gravity
H	height
$\mathbf{j}$	diffusive heat flux
k, $\mathbf{k}$	scalar respectively tensor of permeabilities
k_x, k_z	components of permeability tensor
p	total pressure
Ra	Rayleigh number (see below)
T	temperature
$\mathbf{v}$	Darcy velocity
x	coordinate axis in horizontal direction
z	coordinate axis in direction of gravity.

Greek symbols

γ	ratio of heat capacities $(\rho c)_f/(\rho c)^*$
$\Delta\rho$	density change from upper to lower boundary
φ	porosity
λ	thermal conductivity
μ	dynamic viscosity
θ	normalized temperature
ρ	water density
$(\rho c)_f$	water heat capacity
$(\rho c)^*$	porous medium heat capacity
Ψ	streamfunction.

implies, that density variations can be neglected in the conservation equations. The value for ρ which is used for the calculation of heat and mass flux in each volume element is the same and can be canceled, for it is a multiplier in each equation of the finite formulation.

If the Oberbeck–Boussinesq assumption is valid in the two-dimensional case, the streamfunction Ψ can be introduced to describe the flow field. The flow equation, derived from equations (1) and (3), then reads:

$$\left[\frac{\partial}{\partial x}\frac{\mu}{k_z}\frac{\partial}{\partial x}+\frac{\partial}{\partial z}\frac{\mu}{k_x}\frac{\partial}{\partial z}\right]\Psi=-g\frac{\partial\rho}{\partial x}. \tag{5}$$

The system of equations (2) and (5) is coupled by equations of state, i.e. the temperature dependent fluid characteristics μ and ρ. The functional relationships are discussed below and are shown in Fig. 1. If the porous medium is homogeneous and isotropic, if viscosity is constant and density changes linearly with temperature, a parameter transformation to dimensionless form leads to the following set of equations:

$$\nabla^2\Psi=Ra\frac{\partial\theta}{\partial x} \tag{6}$$

$$\nabla^2\theta-\mathbf{v}\nabla\theta=\frac{1}{\gamma}\frac{\partial\theta}{\partial t}. \tag{7}$$

Wooding [11] and Elder [12] already used this set of equations for their analytical and numerical investigations. In this formulation only one dimensionless constant, derived from the physical parameters remains to describe the whole system. This is the Rayleigh number:

$$Ra=\frac{kg\gamma\,\Delta\rho H}{D\mu}. \tag{8}$$

3. PARAMETER DEPENDENCIES

The system is closed by the equations of state, which describe the temperature dependency of density and viscosity. For density variation as a function of temperature between 0 and 40°C an approximation is given by Tilton and Taylor [13], which is shown in Fig. 1 (top). The well-known anomaly of water is expressed by the fact that the graph has a maximum value at $T=3.98$°C.

As mentioned above the Oberbeck–Boussinesq assumption leads to a simplification of the equations. If the density change is nonlinear, the density derivative on the right hand side of the flow equation is not a constant anymore. This may be interpreted as a locally changing Rayleigh number. On the other hand, if a constant Rayleigh number is defined using the total change of density from the bottom to the top of the system (see equation (8)), a correction factor f_ρ has to be introduced:

$$\nabla^2\Psi=Ra\cdot f_\rho\frac{\partial\theta}{\partial x}$$

with

$$f_\rho=\frac{1}{\Delta\rho}\frac{\partial\rho}{\partial\theta}=\frac{1}{\Delta\rho}\frac{\partial\rho}{\partial T}\frac{\partial T}{\partial\theta}=\frac{T_{\max}-T_{\min}}{\Delta\rho}\frac{\partial\rho}{\partial T}. \tag{9}$$

The correction factor changes with local temperature spatially and temporally. It should be noted, that for temperatures below 4°C f_ρ is negative and positive for temperatures above 4°C—see Fig. 1 (center). In order to estimate the correction factor f_ρ for an arbitrary temperature range $[T_{\min}, T_{\max}]$ one may compare the slope of the density curve with the slope of the line connecting $(T_{\min}, \rho_{\max})$ and $(T_{\max}, \rho_{\min})$ in Fig. 1 (top). Obviously the gradient of the nonlinear curve is smaller for low temperatures, but bigger for

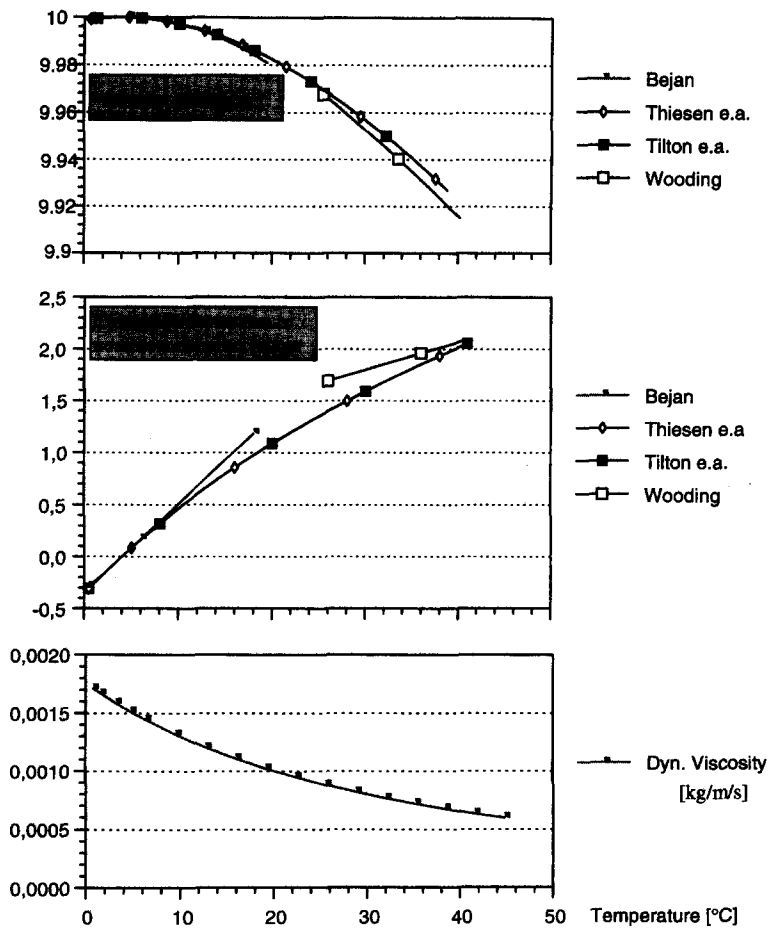

Fig. 1. Density (above), correction factor f_ρ (center) and dynamic viscosity (below) as function of temperature (from: Wooding [11], Tilton and Taylor [13], Thiesen *et al.* [18], Béjan [20] as cited by Nield and Bejan [19]).

high temperatures in the interval $[T_{min}, T_{max}]$. The Rayleigh number will be corrected partly by a factor lower than 1 (in cold water) and partly by a factor greater than 1 (in hotter water).

The changes of dynamic viscosity in the same temperature interval can be described by an exponential relationship given by Yusa and Oishi [14]. A graphical representation is given in Fig. 1 (bottom). Note that the decrease of viscosity is relatively high even for small temperature intervals. From 0 to 20°C the decrease is around 43%. In the temperature range between 4 and 31°C viscosity is reduced by half.

In the same manner a correction factor f_μ is introduced to account for changing viscosity. A reference value for dynamic viscosity μ_{ref} has to be specified in order to calculate the Rayleigh number as a constant characteristic of the system. The correction, which varies with temperature as well, reads:

$$\nabla^2\Psi = Ra \cdot f_\rho f_\mu \frac{\partial\theta}{\partial x} \quad \text{with} \quad f_\mu = \frac{\mu_{ref}}{\mu}. \qquad (10)$$

In correspondence with Kassoy and Zebib [15] the viscosity value at the surface, i.e. for the lowest temperature, is chosen as reference. The product $Ra \cdot f_\rho \cdot f_\mu$ can be understood as a local Rayleigh number. Note, that the influence of pure viscosity changes cannot be studied by this approach: the right side of equation (10) vanishes and the coupling between flow and transport, too. Thus if viscosity effects are mentioned in the following, more precisely the influence of variable viscosity in variable density situations is meant.

Similar to the Oberbeck–Boussinesq assumption for density, a condition for viscosity has to be valid for the above simplification of the flow equation. That is, viscosity variations within one block can be neglected. Changes between blocks have to be considered. The criterion for viscosity is thus not only analytically, but also numerically, determined in so far as the block spacing plays a role. As shown above, a similar argument can be given for the classical Boussinesq–Oberbeck assumption as well.

4. NUMERICAL MODEL

The numerical model is based on a finite difference approximation of the equations (7) and (10). The code FAST-C (two-dimensional) is implemented with the option to switch on/off the two correction terms. The

correction factor accounting for nonlinear density effects is calculated using the approximation given by Tilton and Taylor [13].

All simulations which are reported in the following, are run for a two-dimensional square cavity with equal height and length. The cross-section is divided in 20×20 equidistant blocks. The boundary conditions prescribe a constant value of 0.0 for Ψ on all edges of the boundary, which is the 'no-flow' condition for the fluid in the streamfunction formulation. A high value of 1.0 is prescribed for θ at the upper horizontal boundary, a low value of 0.0 vice versa at the lower horizontal boundary. On the vertical sides the Neumann condition $\partial\theta/\partial x = 0.0$ is used, which demands a zero diffusive heat flux in physical terms. Since there is no advective flux additionally (from the condition for Ψ), this is actually a 'no-flow' condition for heat.

The finite difference method is used for discretization. First-order derivatives are treated by the upwind scheme. Timestepping is done using the Crank–Nicolson method. Timesteps are calculated by the program, taking into account the Courant and Neumann criteria. The same algorithm has been used by Holzbecher and Yusa [16]. Some cases have been run using truncation error correction in order to reduce numerical dispersion. Output comparison indicates deviations as expected; concentration gradients become steeper when the correction scheme is applied. Nevertheless Nusselt numbers are increased only by 1–2% as a result, which was decided to be irrelevant for the work in this study.

Linear systems are solved using preconditioned conjugate gradient methods, the classical algorithm solving for the streamfunction, CGS solving for temperature. The accuracy criterion applied in the linear solvers requires that the maximum change within the last iteration is less than 10^{-5}. Nonlinearity is resolved by introducing an inner (Piccard) iteration, which solves for flow and transport iteratively, until the above mentioned accuracy is reached.

The numerical model simulates the transient behavior of the system. Steady states are approached starting from different initial flow patterns. The criterion for steady state is that the numerical algorithm does not change the streamfunction and temperature distributions within a timestep. This is a numerical criterion, which depends on the accuracy that is required for the linear solvers and on the length of the timestep.

5. STEADY STATE CONVECTION PATTERNS

It is well known from classical theory [1], that the lowest instable mode is two-dimensional. The corresponding eddies have equal length and height, i.e. the aspect ratio H/L is 1. For temperatures above 25°C it has been shown by Kassoy and Zebib [15] that the patterns at the onset of convection remain almost the same, if viscosity changes are taken into account, which are neglected in the classical treatment. A small change in the corresponding wavenumber was detected by Morland *et al.* [17] in the case of nonlinear density changes for temperatures above 25°C.

Convection patterns in cold water convection may be different, as already mentioned by Blake *et al.* [4] and Poulikakos [5]. If low temperatures are below 3.98°C there will be a region near the upper boundary with a stable density gradient. This layer will not be penetrated by convective motions as in the case of overall unstable density gradients. Nevertheless eddies will appear near the upper boundary in supercritical steady state flow.

In this work various flow patterns are investigated, which are derived by introducing perturbations in the initial temperature distribution. The steady state patterns which emerge from these initializations are shown in Fig. 2A–D.

Figure 2A shows a one-eddy pattern, which looks very similar to the patterns shown by Kassoy *et al.* [15]. Nevertheless narrow streamlines are observed in hot water, i.e. near the bottom and in ascending flow. Figure 2B illustrates a two-cell pattern with descending fluid in the middle of the cavity. Both bottom figures show flow patterns with four cells. The upper two cells in Fig. 2C are not visible in the streamfunction plots, which are drawn for a (too) small number of equidistant levels. The $\Psi = 0$ streamline has been added, because it illustrates where the four cells are separated. Nevertheless the emergence of two additional rolls in the 'white spot' region is revealed when a finer scaling for the Ψ-isolines is used. The $\Psi = 0$-isoline separates the convection cells. In both cases, Fig. 2C and D, the upper rolls are much less pronounced than the eddies in the lower part. This can as well be concluded from the fact that the horizontal layering of isotherms is slightly disturbed only. The vertical extension of this upper boundary layer can be attributed to the temperature interval. In Fig. 2C the potentially unstable range extends over 6°C from 10°C total temperature difference, while it is 2°C from a total of 6°C in Fig. 2D.

6. ONSET OF CONVECTION

The onset of convection is investigated by tracing different solution branches with change of parameters. Once a steady state has been reached for a special choice of parameters, the Rayleigh number is reduced successively in small steps. The steady state for the higher Rayleigh number is used as initial state for a simulation run with the lower Rayleigh number. This procedure is repeated until the convection pattern changes or the conductive state is reached.

As a distinction between convective and conductive state the Nusselt numbers are calculated from the steady state temperature fields. More specifically, Nu is determined by use of a third-order extrapolation scheme at both lower and upper boundaries. It could be observed that both values are slightly different for cases which include parameter dependencies on tem-

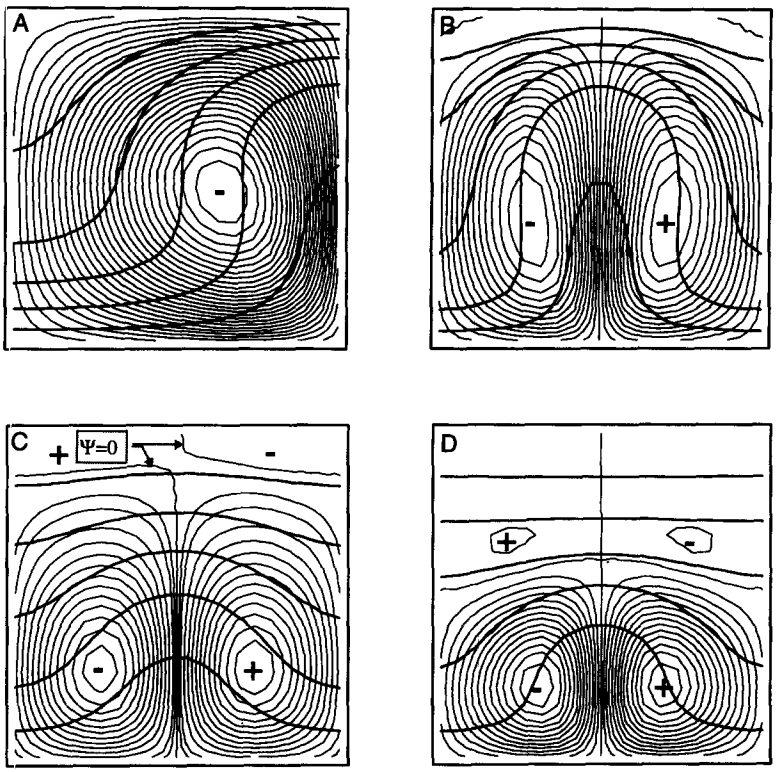

Fig. 2. Steady-state convective flow patterns for cold water in porous medium (streamlines are represented by thin, isotherms by thick lines; signs in eddy centers denote rotational sense: '+' for clockwise and negative Ψ-values, respectively, '−' for counter-clockwise and positive Ψ-values). (A) $T_{min} = 2°C$, $T_{max} = 20°C$, $Ra = 60$, one eddy, $\Psi_{min} = 0.02$, $\Psi_{max} = 4.81$; (B) $T_{min} = 0°C$, $T_{max} = 10°C$, $Ra = 60$, two eddies, $\Psi_{max} = 5.17 = -\Psi_{min}$; (C) $T_{min} = 0°C$, $T_{max} = 10°C$, $Ra = 28.5$, four eddies, $\Psi^1_{max} = 1.52 = -\Psi^1_{min}$, $\Psi^2_{max} = 0.01 = -\Psi^2_{min}$; (D) $T_{min} = 0°C$, $T_{max} = 6°C$, $Ra = 300$, four eddies, $\Psi^1_{max} = 2.99 = -\Psi^1_{min}$, $\Psi^2_{max} = 0.24 = -\Psi^2_{min}$.

perature. Nevertheless the deviations become marginal near the onset of convection. Nusselt numbers reported in this paper are arithmetic means of values calculated at the hot and cold boundaries.

Of interest is the combined effect of the step viscosity gradient on one side, which favors the onset of convection and the nonlinear density change with temperature on the other side, which may hamper the flow development.

6.1. *Low temperatures above 4°C*

The effect of this correction to the onset of convection is marginal as shown in Table 1. The critical values gathered were obtained by the numerical simulation described above with and without correction due to nonlinear density change. The critical values change with temperature because nonconstant viscosity is taken into account. For a different temperature range the effect of reduced critical margins has been reported by Kassoy and Zebib [15], taking into account variable viscosity effects only. Morland *et al.* [17] showed that the critical Rayleigh numbers do not change significantly if nonlinear density changes are considered additionally, for cold temperatures above 25°C.

6.2. *Low temperatures below 4°C*

6.2.1. *High temperatures above 12°C.* If the highest temperatures in the system are above 12°C, the lowest unstable mode remains the one with a single main eddy with aspect ratio ≈ 1. In Fig. 3 the *Ra–Nu*-diagram is given for this convection pattern. Upper boundary temperatures are 0, 2 respectively 4°C; lower boundary temperatures are 12, 20, respectively 40°C.

Table 1. Critical Rayleigh numbers for different temperature ranges with and without consideration of nonlinear density changes

Minimum temperature [°C]	4	4	4	8	8	12
Maximum temperature [°C]	8	12	20	12	20	20
Critical *Ra* number (linear ρ function)	36.5	34.5	31.0	36.5	33.0	35.0
Critical *Ra* number (nonlinear ρ function)	35.5	32.5	28.5	36.5	32.0	34.5

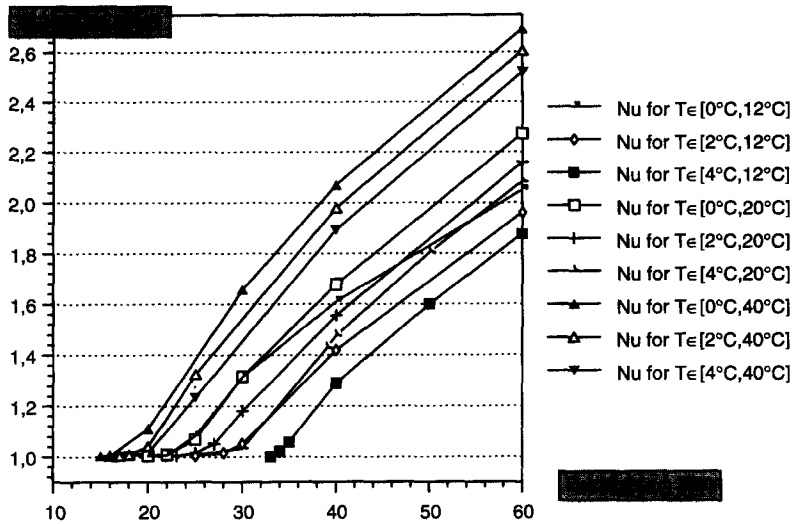

Fig. 3. *Ra–Nu* diagram for low temperatures below 4°C and high temperatures above 12°C.

The figures show that heat transfer changes only slightly with the upper boundary (cold) temperature. For fixed Rayleigh number the Nusselt number decreases if cold temperature at the top is increased. In the constant property case heat transfer would remain the same, thus the difference in heat transfer cannot be explained by the amount of density change from the bottom to the top of the system. An explanation is the variable viscosity (see below).

The critical Rayleigh number for a certain flow pattern is given when, in the tracing procedure described above, the Nusselt number comes down to 1. The marginal state, determined in that way, depends on the specific flow pattern. In order to determine the critical value of *Ra* for the whole system, a variety of convective modes were studied. It turned out that all flow patterns turned into the first mode eddy, when the Rayleigh number was reduced successively. Thus the behavior in general is very similar to the system for temperatures above 25°C, in which Morland *et al.* [17] observed only marginal changes in the convection pattern.

The reduction of the critical Rayleigh numbers is the main fact, which can be recognized in the results given in Fig. 3. The same observation has been made by Kassoy and Zebib [15] for temperatures above 25°C as an effect of variable density and viscosity. The effect is even slightly stronger in cold water. This can be attributed to the fact that absolute change of viscosity is highest for temperatures slightly above the freezing point. Figure 4 provides an overview on critical Rayleigh numbers as function of the temperature range.

6.2.2. *High temperatures below* 10°C. Five temperature intervals have been studied: [0–6°C], [0–8°C], [0–10°C], [2–6°C] and [2–8°C]. The results show a quite different behavior of the system concerning the onset of convection.

In the temperature ranges 0–10°C and 2–8°C the output from the numerical simulations reveals that the one-eddy mode is still the one determining onset of convection (as for temperature intervals with high temperature above 12°C. The critical values of Rayleigh number are 20 respectively 28.5. In the 0–10°C range the four-cell pattern (with two small eddies in the upper and two big eddies in the lower part of the system) breaks down for Rayleigh numbers below 28. In the 2–8°C case a steady-state two-cell pattern (aspect ratio = 0.5) exists, but for Rayleigh numbers above 45 only. From an analytical point of view the four-cell patterns may be identical to the numerically observed two-eddy-system, because the numerical grid may not be able to resolve some details of the flow pattern. This is confirmed by the fact that for higher Rayleigh numbers (>60) the above-mentioned four-cell solution switches to a two-cell solution.

In the temperature intervals 0–6°C, 0–8°C and 2–6°C the four-cell pattern instead seems to be the dominant one near the onset of convection. As can be expected the critical Rayleigh number increases if high temperatures approach 4°C from above, the convective flow hindered when the density difference becomes stabilizing in most parts of the system. For temperatures within the interval 0–6°C perturbations are amplified for Rayleigh numbers above 240 in the described numerical experiments.

The opposite holds in an intermediate range which is represented here by the temperature interval 0–8°C and 2–6°C. The simulations provide critical values of 3.45 for 0–8°C and of 0.11 for 2–6°C. Two explanations can be given for the direction of this effect. At first, the potentially unstable region has a smaller thickness and thus Ra_{crit} becomes smaller, according to classical theory. Secondly, the definition of the Rayleigh number, as given in equation (8), is not convenient any more.

The density difference $\Delta\rho$, used in definition (8), becomes irrelevant in the cold water case. Besides the

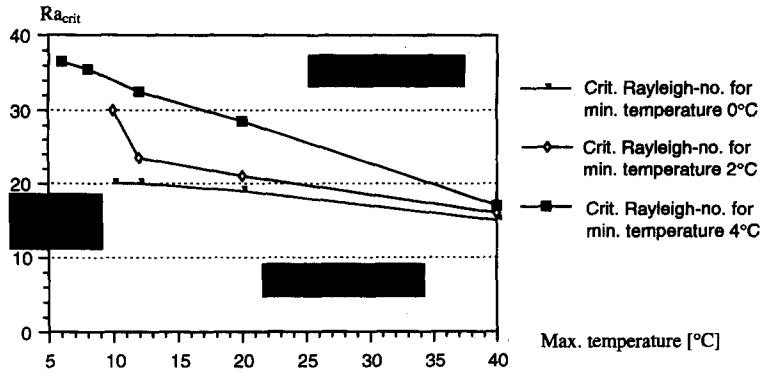

Fig. 4. Critical Rayleigh numbers for different temperature ranges.

fact that it may have the opposite sign in degenerate cases; in the temperature range in question, it underestimates the density changes in the potentially unstable part. While $\Delta\rho$ denotes the water density difference at boundary temperatures, the convective flow is moved by the density difference between 4°C and the temperature at the lower boundary. For that reason Sun *et al.* [2], Yen [3] and Nield and Bejan [19] introduce different definitions for the Rayleigh number of cold water in their studies. These modified values depend strongly on the approximating density function and do not account for variable viscosity as well. The classical definition has been kept in this paper, in order to make comparisons for all temperature ranges and to determine the margin, where the classical approach breaks down.

7. CONCLUSIONS

Rayleigh number correction factors have been introduced into the system of partial differential equations describing density driven flow in two space dimensions. The resulting system then takes into account nonlinear density and viscosity changes. A numerical approach was used to study the effect of these temperature-dependent factors on the onset of convection.

Combined variable density and viscosity effects dominate the onset of convection if high temperatures are above 12°C. The first mode remains to be the effective one at the onset of convection, but critical Rayleigh numbers are lower. The amount of this lowering depends on the temperature difference (Fig. 3). Effects of nonlinear density change cannot be observed in that case. They may be important in temperature ranges with low temperature below 4°C and high temperature below 12°C only.

For cold water with low temperature distinctly below 4°C and high temperature slightly above 4°C the system behaves quite differently, depending on the temperature range. Using the classical definition of the Rayleigh number, the critical margins may be much smaller (temperature intervals 2–6°C and 0–8°C) or much higher (interval 0–6°C) than the classical value of $4\pi^2$. Thus if the temperature interval is centered around 4°C, the critical Rayleigh number is substantially reduced. A shift of the interval towards the freezing point lets the critical margin rise. Remarkable is the emergence of slow convection rolls in the upper part and fast rolls in the lower part of the system, which cannot be observed in systems with linear change of fluid density.

Summarizing it can be stated, that no unique tendency can be observed in the description of thermal convection in cold groundwater. If low temperatures are below 4°C and high temperatures are below 10°C, different phenomena exist concerning the patterns and the margins of criticality.

Acknowledgement—The author is thankful to the 'Deutsche Forschungs Gemeinschaft', which enabled this research by the habilitation grant HO1171/21.

REFERENCES

1. E. R. Lapwood, Convection of a fluid in a porous medium, *Proc. Camb. Phil. Soc. A* **225,** 508–521 (1948).
2. Z. Sun, C. Tien and Y. Yen, Onset of convection in a porous medium containing liquid with a density maximum, in *4th Int. Conf. Heat Transfer*, pp. 2–11, Versailles (1970).
3. Y. Yen, Effects of density inversion on free convective heat transfer in porous layer heated from below, *Int. J. Heat Mass Transfer* **17,** 1349–1356 (1974).
4. K. R. Blake, A. Bejan and D. Poulikakos, Natural convection near 4°C in a water saturated porous layer heated from below, *Int. J. Heat Mass Transfer* **27,** 2355–2364 (1984).
5. D. Poulikakos, Onset of convection in a horizontal porous layer saturated with cold water, *Int. J. Heat Mass Transfer* **28,** 1899–1905 (1985).
6. M. A. Combarnous and S. A. Bories, Hydrothermal convection in saturated porous media, *Adv. Hydrosci.* **10,** 231–307 (1975).
7. D. D. Joseph, *Stability of fluid motions*, II. p. 274. Springer, Berlin (1976).
8. A. Oberbeck, Ueber die Wärmeleitung der Flüssigkeiten bei Berücksichtigung der Strömungen infolge von Temperaturdifferenzen, *Ann. Phys. Chem.* **7,** 271–292 (1879).
9. J. M. Mihaljan, The rigorous exposition of the Boussinesq approximations applicable to a thin layer of fluid, *Astrophys. J.* **136,** 1126–1133 (1962).
10. P. C. Fife, The Bénard problem for general fluid dynamical equations and remarks on the Boussinesq approximation, *Indiana Univ. Math. J.* **20,** 303–326 (1970).

11. R. A. Wooding, Steady state free thermal convection of liquid in a saturated permeable medium, *J. Fluid Mech.* **2,** 273–285 (1957).
12. J. W. Elder, Transient convection in a porous medium, *J. Fluid Mech.* **27,** 609–623 (1967).
13. L. W. Tilton and J. K. Taylor, Accurate representation of the refractivity and density of distilled water as a function of temperature, *J. Res. Nat. Bur. Stand.* **18,** 205–214 (1937).
14. Y. Yusa and I. Oishi, Theoretical study of two-phase flow through porous medium (II), *J. Geotherm. Res. Soc. Jap.* **11,** 217–237 (1989).
15. D. R. Kassoy and A. Zebib, Variable viscosity effects on the onset of convection in porous media, *Phys. Fluids.* **18,** 1649–1651 (1975).
16. E. Holzbecher and Y. Yusa, Numerical experiments on free and forced convection in porous media, *Int. J. Heat Mass Transfer* **38,** 2109–2115 (1995).
17. L. W. Morland, A. Zebib and D. R. Kassoy, Variable property effects on the onset of convection in an elastic porous matrix, *Phys. Fluids* **20,** 1255–1259 (1977).
18. Thiesen, Scheel and Distelhorst, *Wiss. Abhandlungen Phys. Techn.* Reichsanstalt 3, p. 67 (1900).
19. D. A. Nield and A. Bejan, *Convection in Porous Media*, Springer, New York (1992).
20. A. Bejan, Convective heat transfer in porous media, in: *Handbook of Single-Phase Convective Heat Transfer* (Edited by S. Kakaç, R. K. Shah and W. Aung). Wiley, New York (1987).

APPENDIX

The derivation of equations (6)–(8) are from basic laws (1)–(4). The streamfunction Ψ is introduced using the defining equations with the components of Darcy velocity v_x and v_z:

$$\frac{\partial \Psi}{\partial x} = v_z \quad \frac{\partial \Psi}{\partial z} = -v_z.$$

Using these equations and Darcy's Law (3) with permeabilities k_x respectively, k_z for horizontal and vertical direction the following differential for the streamfunction is obtained (mixed pressure derivatives with different sign cancel):

$$\frac{\partial}{\partial x}\frac{\mu}{k_z}\frac{\partial \Psi}{\partial x} + \frac{\partial}{\partial z}\frac{\mu}{k_x}\frac{\partial \Psi}{\partial z} = \frac{\partial}{\partial x}\frac{\mu}{k_z}v_z - \frac{\partial}{\partial z}\frac{\mu}{k_x}v_x = -g\frac{\partial \rho}{\partial x}.$$

Local changes in viscosity can be neglected—in analogy to the Boussinesq–Oberbeck assumption for density (see part 1). For constant permeability $k_x = k_z = k$ results in a potential equation type equation for Ψ:

$$\frac{\partial^2 \Psi}{\partial x^2} + \frac{\partial^2 \Psi}{\partial z^2} = -\frac{kg}{\mu}\frac{\partial \rho}{\partial x}. \tag{A1}$$

Fourier's law (4) is introduced in the transport equation (2).

$$\frac{\partial}{\partial t}(\rho c)^* T = -\nabla[(\rho c)_f \mathbf{v} T - \lambda \nabla T].$$

If local (spatial and temporal) changes in heat capacity are neglected, the following is obtained:

$$\frac{\partial T}{\partial t} = -\gamma \nabla \mathbf{v} T + \frac{\lambda}{(\rho c)^*}\nabla^2 T.$$

The coefficient of $\nabla^2 T$ is the thermal diffusivity D. For the normalized temperature $\theta = (T - T_{\min})/(T_{\max} - T_{\min})$ holds:

$$\frac{1}{D}\frac{\partial \theta}{\partial t} = -\frac{\gamma}{D}\nabla \mathbf{v}\theta + \nabla^2 \theta. \tag{A2}$$

As next step, streamfunction and velocities are transformed using the following rules:

$$\Psi \to \frac{D}{\gamma}\Psi \quad \mathbf{v} \to \frac{D}{\gamma}\mathbf{v}$$

and for the system of equations (A1) and (A2) results:

$$\frac{\partial^2 \Psi}{\partial x^2} + \frac{\partial^2 \Psi}{\partial z^2} = -\frac{kg\gamma}{\mu D}\frac{\partial \rho}{\partial x}$$

$$\frac{1}{D}\frac{\partial \theta}{\partial t} = -\nabla \mathbf{v}\theta + \nabla^2 \theta.$$

Here again local changes of diffusivity and the heat capacity ratio are neglected. The classical flow equation (6) follows under the assumption of a linear density relation $\rho = \rho_0 - \theta \Delta\rho$. Additionally the lengths need to be scaled to the height H of the system: $x \to x/H$, $z \to z/H$.

$$\nabla^2 \Psi = \frac{kg\gamma \Delta\rho H}{\mu D}\frac{\partial \theta}{\partial x}.$$

The combination of parameters appearing as coefficient on the right hand side of the equation, is the dimensionless Rayleigh number.

The transport equation as stated in equation (7), follows using the continuity equation $\nabla \mathbf{v} = 0$, which holds when the Boussinesq–Oberbeck assumption is valid:

$$\frac{1}{DH^2}\frac{\partial \theta}{\partial t} = -\mathbf{v}\nabla\theta + \nabla^2 \theta.$$

Transforming time by $t \to tDH^2/\gamma$ finally provides the aimed (dimensionless) formulation.